 doi:10.20944/preprints201608.0069.v1

Article

Comparison of Pixel- and Object-Based Approaches in Phenology-Based Rubber Plantation Mapping in Fragmented Landscapes

Deli Zhai [1,2], Jinwei Dong [3], Georg Cadisch [4], Mingcheng Wang [1,2], Weili Kou [3,5], Jianchu Xu [1,2,*] and Xiangming Xiao [3,6,*]

1 Key Laboratory for Plant Diversity and Biogeography of East Asia (KLPB), Kunming Institute of Botany, Chinese Academy of Sciences, 132 Lanhei Road, Kunming 650201, Yunnan, China; zhaideli@mail.kib.ac.cn (D.Z.); wangmingcheng@mail.kib.ac.cn (M.W.)
2 World Agroforestry Centre, East and Central Asia Office, 132 Lanhei Road, Kunming 650201, Yunnan, China
3 Department of Microbiology and Plant Biology, and Center for Spatial Analysis, University of Oklahoma, Norman, OK 73019, USA; jinwei.dong@ou.edu
4 Plant Production in the Tropics and Subtropics (380a), University of Hohenheim, Garbenstrasse 13, 70599 Stuttgart, Germany; georg.cadisch@uni-hohenheim.de
5 School of Computer Science and Information, Southwest Forestry University, Kunming 650224, Yunnan, China
6 Institute of Biodiversity Science, Fudan University, Shanghai 200433, China
* Correspondence: J.C.Xu@cgiar.org (J.X.); xiangming.xiao@ou.edu (X.X.); Tel.: +86-871-6522-3052 (J.X.); +1-405-325-8941 (X.X.); Fax: +86-871-6521-6350 (J.X.); +1-405-325-3442 (X.X.)

Abstract: Effectively mapping and monitoring rubber plantation is still changing. Previous studies have explored the potential of phenology features for rubber plantation mapping through a pixel-based approach (pixel-based phenology approach). However, in fragmented mountainous Xishuangbanna, it could lead to noises and low accuracy of resultant maps. In this study, we investigated the capability of an integrated approach by combining phenology information with an object-based approach (object-based phenology approach) to map rubber plantations in Xishuangbanna. Moderate Resolution Imaging Spectroradiometer (MODIS) data were firstly used to acquire the temporal profile and phenological features of rubber plantations and natural forests, which delineates the time windows of defoliation and foliation phases. Landsat images were then used to extract a phenology algorithm comparing three different approaches: pixel-based phenology, object-based phenology, and extended object-based phenology to separate rubber plantations and natural forests. The results showed that the two object-based approaches achieved higher accuracy than the pixel-based approach, having overall accuracies of 96.4%, 97.4%, and 95.5%, respectively. This study proved the reliability of a phenology-based rubber mapping in fragmented landscapes with a distinct dry/cool season using Landsat images. This study indicated that the object-based phenology approaches can effectively improve the accuracy of the resultant maps in fragmented landscapes.

Keywords: Rubber (*Hevea brasiliensis)* plantation; phenology; Xishuangbanna; Landsat; object-based approach; pixel-based approach

 doi:10.20944/preprints201608.0069.v1

1. Introduction

Tropical regions are being increasingly covered by monoculture plantations [1,2]. For example, rubber (*Hevea brasiliensis*) plantations have expanded greatly in recent decades and have been a critical driver of land cover change around the world, especially in Southeast Asia[2]. The global rubber plantation area has steadily increased by 25% during the past two decades [3] while around 97% of global natural rubber supply is from Southeast Asia [4], with the vast majority coming from Thailand (31%), Indonesia (30%), and Malaysia (9%) in 2010.It is projected that the global demand for natural rubber will further increase from 9.6 million tons in 2008 to 13.8 million tons by 2018 [5]. The expansion of rubber plantations has been a primary driving factor of deforestation and decreasing of swidden agricultural lands in Southeast Asia [6,7]. Even the northern part of the tropical belt, which was originally unsuitable for rubber plantation planting (such as Xishuangbanna in China) has recently been occupied by substantial rubber plantations due to use of cold-tolerant tree clones[8]. This change in rubber plantation magnitude and extent has economic, social, and environmental impacts. The increasing rubber plantation areas could benefit the local economy and farmer incomes [9], but at the cost of disrupting traditional lifestyles, as well as indigenous ecological knowledge, aesthetic, and cultural practices [8,10]. Ecologically, the expansion of rubber plantations has caused a series of environmental issues such as reducing concentrations of soil organic carbon, carbon storage, and local biodiversity, and has resulted in reduced stream flows and water storage in the dry season[2,11,12], which has greatly changed regional environment and ecosystem services. To better examine the ecological, social and economic impacts of rubber plantation, improved accurate spatial datasets of the distribution and changes of rubber plantations are needed.

However, existing knowledge and data of rubber plantation area dynamics and spatial patterns are not sufficient to support in depth economic, social, and environmental studies, especially in the northern border of tropical regions in Southeast Asia and China [13].The rapid growth of rubber plantations in the Xishuangbanna Region of Yunnan Province in China, by displacing traditional agriculture and natural forest [4,14],has received much attention[2,15]. Accurate mapping and monitoring rubber plantations in Xishuangbanna is therefore crucial to quantify and project the ecological and socio-economic impacts of rubber plantation expansion.

Great efforts have been devoted to map rubber plantations in the past, which can be generally divided into two groups. One group of studies mapped rubber plantations using an image statistic approach and single-date satellite images, usually at moderate spatial resolution (tens of meters). For example, Landsat TM (Thematic Mapper) and ETM+ (Enhanced Thematic Mapper) have been widely used to delineate rubber plantation distribution[7,12,16-18]. However, frequent cloud cover and limited data acquisition (16-day revisit interval by Landsat) in tropical regions often results in few cloud-free Landsat images available, and that constrains rubber plantation mapping in tropical regions. Additionally, spectral characteristics of rubber plantations vary in different regions and with seasons, and can exhibit similar spectral characteristics as natural forest in a single image captured during the growing season [19,20]. The other group of studies used time series image analysis or a phenology-approach to map rubber plantations. For example, Moderate Resolution Imaging Spectroradiometer (MODIS)sensor and China's Feng-Yun-3A (FY-3A) have been used to map rubber plantations with temporal signals from the images and the intra-annual temporal features or phenological characteristics of rubber plantations have been used to extract rubber plantation locations[21-23]. For example, [22]revealed that rubber plantations have two unique stages (defoliation and foliation) given their deciduous characteristics in northern tropical areas. Rubber plantations and natural forests can be separated effectively during those two phases. [23]also examined phenological metrics of rubber plantations and other land covers, and then conducted classification based on the phenology signatures. The results

revealed that phenological characteristics are very useful for rubber plantation and natural forest mapping in tropical China. However, the coarse spatial resolution of MODIS limits its suitability for rubber plantation mapping in fragmented landscapes like Xishuangbanna [19].

To overcome the limitations mentioned above, researchers tried to use cloud-free sensors or used phenological information of different forest types at certain phenological phases to facilitate rubber plantation and other forest type classification. For example, two studies used Advanced Land Observing Interferometric Synthetic Aperture Radar (ALOS PALSAR) to acquire a forest mask, and then applied the phenology variable derived from Landsat to separate natural forests and rubber plantations[19,22]. The integration of Landsat and PALSAR overcame the mixed pixel problem of MODIS and made progress in rubber plantation mapping. This method of combining PALSAR with Landsat was proven effective in Hainan with relatively smooth terrain[19,22]; however, its application in Xishuangbanna is more challenging given the dramatically fragmented landscapes, as the complex and mountainous landscapes in Xishuangbanna could cause more noises in PALSAR data.

Two aspects of improvement are expected in this study. First, is the solution to resolve the relying on PALSAR for the resultant thematic map relying on RADAR (PALSAR) in this study might result in decreasing the accuracy as the complex and mountainous terrain in Xishuangbanna could cause more noise for RADAR data. It would be important to explore whether optical imagery (i.e. Landsat) alone is sufficient to map rubber plantations in highly fragmented and heterogeneous landscapes. Second, we assumed an object-based approach could improve the accuracy of the pixel-based phenology approach in the previous study [19] for mountainous Xishuangbanna area, as the object-related approach has been proven useful in identification large-scale artificial objects [24-26] e.g. assisting the identification of rubber plantations[17].

The objective of this study is to improve the existing phenology-based rubber plantation mapping algorithm using object-based approaches. Specifically, we try to answer two questions regarding mapping rubber plantations: 1) Is the phenology-based approach of rubber plantation effective and robust in mountainous Xishuangbanna? 2) Can a combined object- and phenology-based approach improve the delineation of rubber plantations compared to pixel- and phenology-based approach? To achieve this objective we integrated ground observational data and Landsat imagery to examine the phenology signatures of rubber plantations, and compare three different approaches (a pixel-based phenology approach, an object-based phenology approach based on thresholds, and an extended object-based phenology approach by using multiple phenology related variables and object-based classification). This study is expected to provide a general practical approach for regional rubber plantation mapping applicable in southern China and Southeast Asia in the near future.

2. Materials and Methods

2.1. Study area

Xishuangbanna Dai Nationality Autonomous Prefecture (21°08'–22°36' N, 99°56'–101°50' E, Fig.1) in Yunnan Province, southwest China, covers 19,150 km^2, and lies within the Indo-Burma global biodiversity hotspot area [27]. It borders Laos to the south and Myanmar to the southwest. The elevation varies from 475 to 2,430 m above sea level, and about 95% of the region is covered by mountains and hills. Despite its high latitude and elevation, Xishuangbanna has a tropical moist climate in the southern area due to a barrier effect caused by the Hengduan Mountains which hold off cold air from the north during winter [28]. Therefore, the climate in Xishuangbanna is influenced by continental air masses in winter and warm-wet air masses from the Indian Ocean in summer. This gives rise to a summer monsoon with a rainy season from May to October and thereafter a dry season from November to April

Preprints (www.preprints.org) | NOT PEER-REVIEWED | Posted: 6 August 2016 doi:10.20944/preprints201608.0069.v1

which includes a cool dry season from November to February characterized with cool temperature (15.9˚C the coldest) and a hot dry season from March to April characterized with relatively hot temperature (above 38˚C) and low relative humidity (less than 40% vs. the mean monthly relative humidity of 87%) [29]. The dry season is characteristic for relatively less rainfall, low temperatures, and fog which take up about 37% of the time in dry season. Heavy fog occurs overnight until the next morning in the cool dry season, and the hot dry season is dry and hot during the afternoon, with fog occurring in the morning only [30].There are four major forest types: tropical rain forest, tropical seasonal moist forest, tropical monsoon forest, tropical montane evergreen broad-leaved forest[28]. Only the tropical monsoon forest is a deciduous forest, and the others are evergreen forests.

Rubber trees(*Hevea brasiliensis*) are native to the tropical rainforest of the Amazon Basin, and were not introduced into Xishuangbanna until 1940s[31]. When rubber trees were first introduced, they were considered unsuitable for northern marginal parts of the tropics such as Xishuangbanna with cool winters and a distinct dry season [19]. Hence, hybrid rubber trees were developed and then adapted to the local climate[4]. In contrast to rubber trees in the Amazon, rubber trees in Xishuangbanna shed leaves in the coldest and driest months (January to March) and then undergo a rapid refoliation period [32].

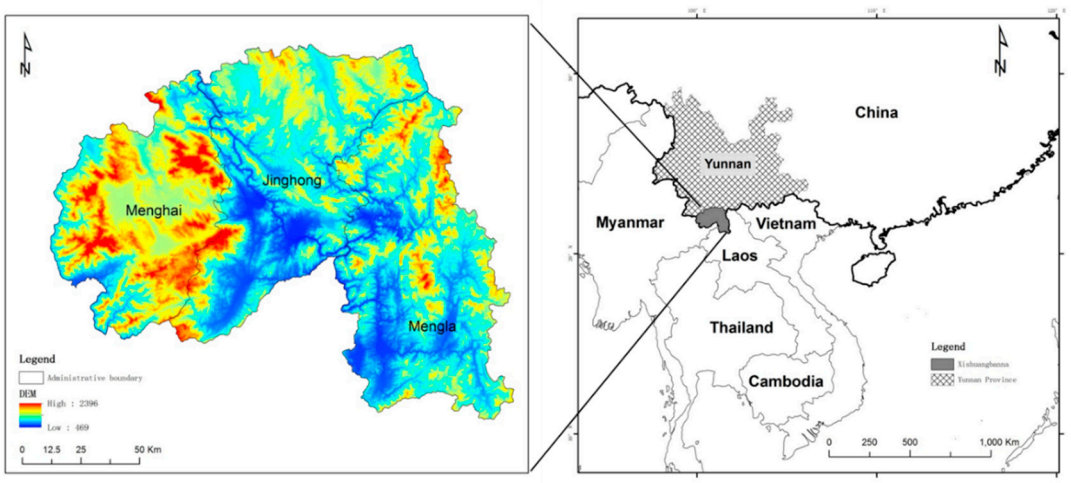

Fig. 1. Location of Xishuangbanna(XSBN) in mainland Southeast Asia and its elevation.

2.2. Landsat data and preprocessing

In order to capture phenological characteristics of defoliation/refoliation of rubber trees from previous MODIS analysis (Fig. 2), 11 standard level-one terrain-corrected(L1T) products of Landsat Thematic Mapper (TM) and Enhanced Thematic Mapper Plus (ETM+) images (path/row 130/45)from 2002 to 2003 were obtained from the USGS Earth Resources Observation and Science (EROS) Data Center (Table 1) by filtering images from Day of the Year(DOY) 7 to DOY 119.In this research, we used Landsat 5 TM and Landsat 7 ETM+ with a pixel resolution of 30m for reflective bands and 120m for thermal bands (Table S1). As the scan-line corrector (SLC) onboard Landsat 7 failed on May 31, 2003, the images acquired by Landsat 7 called SLC-off have a duplicated area, particularly within the central part of any given scene. Therefore, to obtain more images from January to April, we used data before Landsat 7 SLC-off.

Preprints (www.preprints.org) | NOT PEER-REVIEWED | Posted: 6 August 2016 doi:10.20944/preprints201608.0069.v1

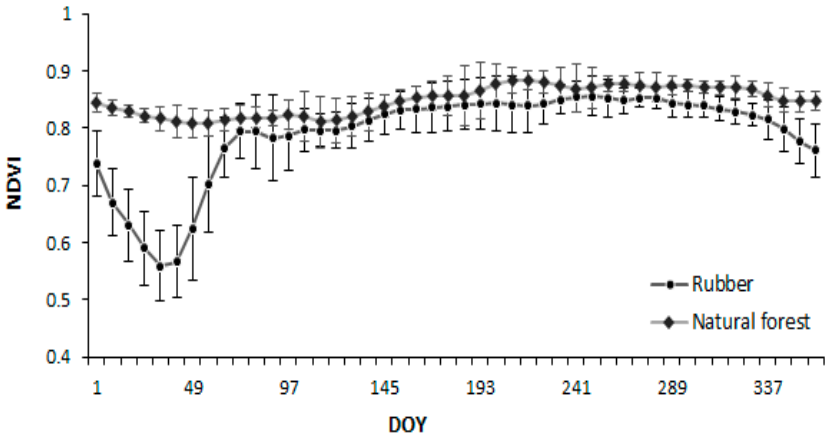

Fig.2. Temporal profiles of time series MODIS NDVI(Normalized Differential Vegetation Index) for natural forests and rubber plantations from 2001-2010, with error bars representing standard deviation.

Table 1. A list of Landsat TM/ETM+ images with the same orbit number (Path/Row 130/45) selected for this study.

Acquired data	DOY	Sensor	Acquired year
January 7	7	Landsat 5 TM	2002
January 26	26	Landsat 5 TM	2003
February 8	39	Landsat 5 TM	2002
February 11	42	Landsat 5 TM	2003
February 19	50	Landsat 7ETM+	2003
February 28	59	Landsat 5 TM	2003
March 4	63	Landsat 7ETM+	2002
March 28	87	Landsat 5 TM	2002
April 8	98	Landsat 7ETM+	2002
April 21	111	Landsat 7ETM+	2002
April 29	119	Landsat 5 TM	2002

In these 11 Level 1Terrain Corrected (L1T) Landsat products, a series of preprocessing have been done by USGS, including radiometric and geometric corrections have been conducted, and the overall geometric fidelity has also been fitted using ground control points and a digital elevation model (DEM)[33,34].Therefore, we only conducted atmospheric correction and acquired surface reflectance by using the Landsat Ecosystem Disturbance Adaptive Processing System (LEDAPS) routine, which uses the MODIS 6S radiative transfer approach to retrieve surface reflectance [35,36]. Three vegetation indices with two canopy greenness vegetation indices and one moisture-related vegetation index were used in this research to capture the seasonal changes of rubber plantation and natural forests. Three vegetation indices (VIs) were selected based on our previous knowledge of rubber plantations in northern parts of tropical Asia [19,22,37]: the Normalized Differential Vegetation Index (NDVI) [38]could extract cannopy greenness or the amount of vegetation, the Enhanced Vegetation Index(EVI)shows higher resistance in atmospheric aerosol variations and soil background than NDVI [39], and the Land Surface Water Index(LSWI)is more sensitive to moisture of land surface and leaf water content[40] were calculated from Landsat data with the following formulas:

Preprints (www.preprints.org) | NOT PEER-REVIEWED | Posted: 6 August 2016 doi:10.20944/preprints201608.0069.v1

$$\mathrm{NDVI} = \frac{\rho_{nir} - \rho_{red}}{\rho_{nir} + \rho_{red}} \quad (1)$$

$$\mathrm{EVI} = 2.5 \times \frac{\rho_{nir} - \rho_{red}}{\rho_{nir} + 6 \times \rho_{red} - 7.5 \times \rho_{blue} + 1} \quad (2)$$

$$\mathrm{LSWI} = \frac{\rho_{nir} - \rho_{swir1}}{\rho_{nir} + \rho_{swir1}} \quad (3)$$

where ϱ_{blue}, ϱ_{red}, ϱ_{nir}, and ϱ_{swir1} are the reflectance values of the Band 1 (Blue, 450–520nm), Band 3 (Red, 630–690nm), Band 4 (NIR1, 760–900nm) and Band 5 (Shortwave-infrared, SWIR for short hereafter, 1,550–1,750nm) in Landsat TM/ETM+ sensors, respectively. And for EVI, the canopy background adjustment factor is 1, and 6 and 7.5 are the aerosol resistance weights.

2.3. Training and validation data collection and field observations of rubber plantation phenology

Rubber plantation and natural forests ground truth and validation data in a stratified random sampling with a Global Position System receiver (Garmin eTrex) were collected by field surveys in 2011 and 2012. We converted all these GPS points data (.shp) to .kml files, which were then used as points of interests (POIs). All these POIs were then digitized to regions of interest (ROIs) in Google Earth (GE) for training and thematic layer validation (Fig. 3). The ROIs were extrapolated from POIs by linking the same period of high spatial resolution images in Google Earth (using historical imagery bar)and then digitalized the POI located homogeneous patch to ROI, which has been proven to be an effective approach and could also generate more training and validation data[19], and the geometric accuracy of GE has been proved in previous study [41].

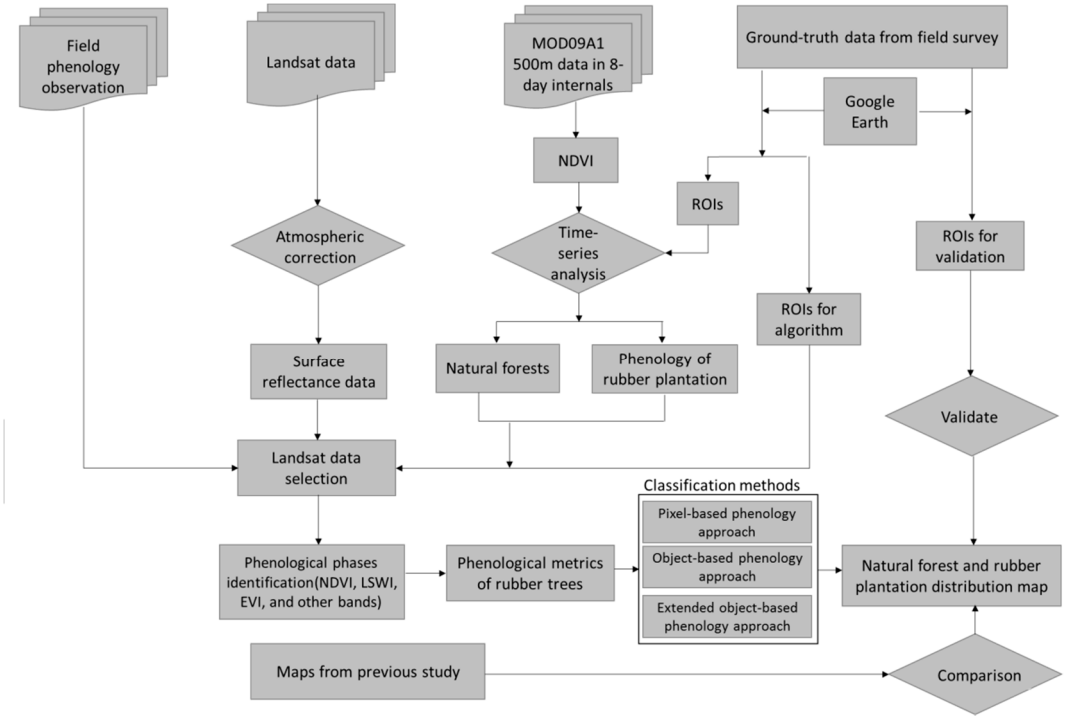

Fig.3. The workflow for mapping rubber plantation based on 500 m MODIS MOD09A1 product and 30 m Landsat images. MODIS-based time-series analysis was used to extract distinct phenological time phase information and based on this Landsat images were selected and further analyzed for specific signatures. A group of ROIs was then developed as training samples for the phenology feature analysis of rubber plantation (11 rubber ROIs, 37,559pixels) and natural forest (11 natural forest ROIs, 123,025pixels).

 doi:10.20944/preprints201608.0069.v1

Three groups of ground truth data were used: (a) the ROIs were used for the phenology phase (2001-2011) extraction (11 natural forests and 11 rubber plantations) by using MODIS, (b) the training ROIs were used to acquire the phenological features of rubber plantations based on the Landsat images during the foliation stage and defoliation stage, and (c) the validation ROIs (30 rubber plantations) were used for accuracy assessments of the derived natural forests (16 from Google Earth) and the rubber plantation map.

Field observations were conducted at a site in Xishuangbanna (101°16'1. 43"E, 21°54'30. 23"N)in order to observe the phenological developments of rubber trees. The site was visited twice a month, and photos were taken using a digital camera every visit to record the phenological conditions(including litterfall) of rubber trees (Fig. 4).

We used MODIS time series data to acquire phenological characteristics of rubber plantations given its higher temporal resolution and data availability. The MODIS data were downloaded from the NASA Land Processes Distributed Active Archive Center (LP DAAC)(http://lpdaac.usgs.-gov/products/). The NDVI was selected based on our previous experiences and the special phenological features of rubber in northern marginal parts of tropical Asia [19,22,37] (Fig. 2).

Previous research indicates that differences in temporal profiles of NDVI values between rubber plantations and natural forests were significantly larger than that of corresponding EVI and LSWI values[22]. Therefore, in the present research the 500m MOD09A1 NDVI products from 2001 to 2011 were constructed to identify and examine the phenology of rubber trees and natural forests (Fig. 2). Temporal profiles of NDVI from MODIS over eight sampling sites (eight of the 11 samples) with rubber trees older than 25 years were collected from rubber plantations and another eight sites for natural forests. The average NDVI value of rubber plantations decreased substantially from late October to early February of the following year, and the lowest NDVI values appeared in January and February (Fig. 2), during the non-growing season. With beginning of the growing season, NDVI increases rapidly from mid-February to October (Fig. 2). Based on this intra-annual temporal analysis of NDVI, we concluded that rubber plantations and natural forests can be clearly distinguished by MODIS (Fig.2)during two periods: 1) early January to early February (defoliation period) and 2) February to early March (foliation period).

Preprints (www.preprints.org) | NOT PEER-REVIEWED | Posted: 6 August 2016 doi:10.20944/preprints201608.0069.v1

Fig. 4. Observed temporal changes of a rubber plantation in Xishuangbannaduring 2013-2014.

Based on the above, previous findings of defoliation and foliation periods, two Landsat images (Path/Row 130/45) with one in the defoliation period (February 19th, 2003) and the other one in the foliation period (April 21st, 2002)were selected from the available eleven images. The selected images covered 87.3% of the total prefecture of Xishuangbanna (16,727 km^2vs. 19,150 km^2 of the total prefecture). The first two images clearly showed differences in the false color composite map(R/G/B=Band 5/4/3), with pink indicating the rubber defoliation period and light green during the foliation period of rubber **(**Fig. 5a+b**)**. We found that images from these unique phenological phases have better separation performance than those taken during the growth phase **(**Fig. 5c**)**(the value of rubber plantation and natural forests are not overlapping and showed higher difference which is also called higher separability performance in this study). For example, rubber plantations and natural forests have similar optical characteristics in an image acquired in November (Fig. 5c). The three vegetation

Preprints (www.preprints.org) | NOT PEER-REVIEWED | Posted: 6 August 2016 doi:10.20944/preprints201608.0069.v1

indices (NDVI, EVI, and LSWI) and the six spectral bands (Blue, Green, Red, NIR, SWIR1, and SWIR2) of both Landsat images(the images acquired in February 19th, 2003 and April 21st, 2002, see 2.6 for details) were stacked for phenology feature extraction of rubber plantations.

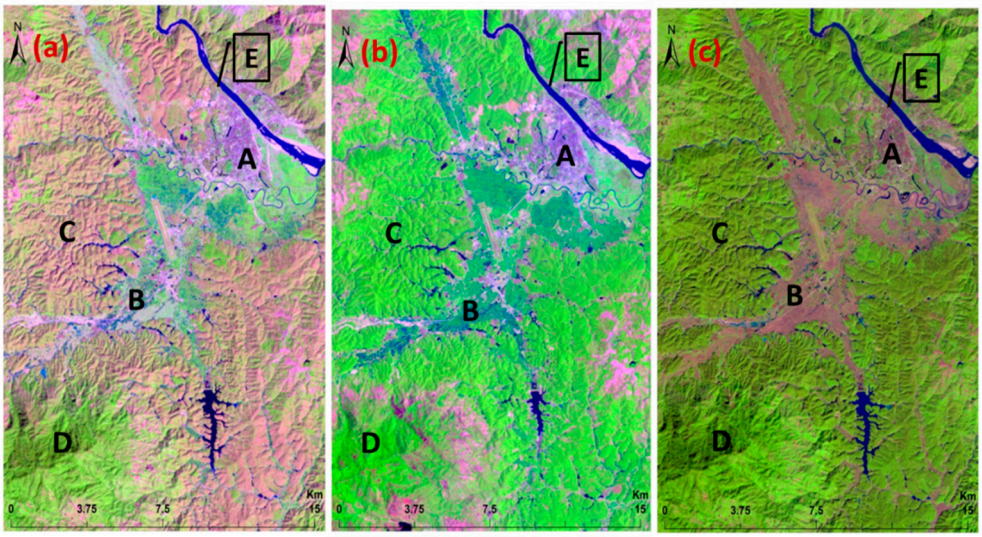

Fig.5. False color composition map (R/G/B = Band 5/4/3) of Landsat images (a) —February 19th, 2003, (b) —April 21st, 2002, and (c) November 20th, 2001. The below images of a small area show that rubber plantation is readily visible as light green patches in the foliation stage image (a), but rubber plantation and natural forest are indistinguishable in (c) which is in neither defoliation nor foliation stage. Several classes of interest were marked in the images, including built-up land (A), agricultural land (B), rubber plantation(C), and natural forest (D), and waterbody (E).

2.4. Mapping rubber plantations using phenology at regional scale

The rubber plantation and natural forest distribution map were classified by using three approaches. The first approach was the phenology-based classification at pixel-level by using threshold-based segmentation as stated by Dong, *et al.* [19] (hereafter, 'pixel-based phenology approach'). The second approach additionally used threshold-based and object-based segmentations units (hereafter, 'object-based phenology approach'). The third approach was also object and phenology based but we considered more variables including VIs algorithms of defoliation and foliation (hereafter, 'extended object-based phenology approach'). Both object-based results were derived by using eCognition (an object-based classifier)(Version 8.0, Trimble).The thematic maps from the last two approaches included three classes: natural forests, rubber plantations, and other land use types.

2.4.1.Pixel-based phenology approach

The pixel-based phenology approach was conducted by using a threshold-based classification and combining Landsat and PALSAR imagery[19,42]. The structure information extracted from L-band PALSAR data was used to generate a tree baseline map and then the phenology information from time series Landsat imagery was taken into account to discriminate natural forests and rubber plantation. Specifically, the forest baseline map was derived by using threshold-based approach and the 50-m PALSAR data. HH and HV polarization backscatters and the ratio (difference) of HH and HV were considered in the process. According to MODIS-based temporal profile analysis, we found the defoliation and foliation phases of rubber plantations were early January to early February and February to

Preprints (www.preprints.org) | NOT PEER-REVIEWED | Posted: 6 August 2016 doi:10.20944/preprints201608.0069.v1

early of March respectively. The two periods of images were used and the mean and standard deviation values were calculated to set the threshold values for the classification between natural forests and rubber plantation. In the foliation phase NIR reflectance was selected to separate rubber plantations from natural forests, while NDVI and LSWI were selected during the defoliation phase. Based on samples gathered from the fields and Google earth, thresholds of NIR, NDVI, or LSWI were set by statistics method. According to the threshold, rubber plantations were extracted from the forest baseline map.

2.4.2.Object-based phenology approach

The object-based phenology approach was carried at two levels of object-based classification. The main part of object-based classification was segmentation, by segmentation the pixels of the image would be first aggregated into homogenous units according to statistic and texture calculation then be subdivided into objects. The multi-resolution segmentation, a bottom-up homogenous region aggregation technique based on certain criteria (e.g. scale, shape, and compactness criteria)[43] was selected for this research.The scale parameter determines the size of objects or the homogenous for the derived image objects[43].Actually, it is not possible to determine directly the correct scale parameter for analysis, and different scale parameters will have different significant objects [43]. Due to the merging objects, scale and shape of the objects are empirically determined by analysts [44-46], specifically, several experiments with different scales were tested and repeated for specific classification objects combined with our local expert knowledge [14,43,44,46,47].The shape weight of input image layers contributing to image segmentation was assigned to 0.1, which meant the color weight was 0.9. The compact parameter shows a relatively against relationships with smoothness, and we used 0.5 for it. All non-thermal bands of Landsat images (six bands) were used for image segmentation, therefore twelve bands as we used images in both defoliation stage and foliation stage. Then we derived classes using the hierarchy approach (Table 2), and all the objects in different scale from previous segmented could be meaningful linked by a hierarchy approach.

Table 2. The multiresolution segmentation parameters

Multi-resolution segmentation					Classification	
Segment level	Scale	Shape	Compactness	Classes	Object-based Phenology approach	Extended object-based Phenology approach
Level1	20	0.1	0.5	Vegetation/Non-vegetation	Nearest Neighbor classifier	
				Nodata	Membership Function classifier	
Level2	10	0.1	0.5	Natural forests/Rubber Plantations	Decision tree classifier	Nearest Neighbor classifier
				Water bodies/ other land use types	Membership Function classifier	Membership Function classifier

The first level classes(i.e. vegetation, non-vegetation, and nodata) were classified at the highest image object level with a coarse scale (20 in Table 2).More detailed classes were further defined at the second object level with a finer scale(10 in Table 2). The second level with its parent level vegetation was classified into natural forests, rubber plantations, and other land use types. For both object-based approaches, the first level used the same classification to classify the image objects into vegetation and non-vegetation using Nearest Neighbor classifier, and nodata by membership function. The membership function is an algorithm in eCognition using fuzzy logic that determines the degree of membership of

 doi:10.20944/preprints201608.0069.v1

image objects to a class and also to define the relationship between feature values (Table2). The membership function was adopted because expert knowledge is crucial for it and better expert knowledge could result in better classification. At the second level, both object-based approaches used membership function classifier to classify water body and other land use types, while for the separation of natural forests and rubber plantations were different for the two different object-based approaches. The object-based phenology approach applied decision tree classifier same as that of pixel-based phenology approach. We used decision tree classifier to insert threshold condition to the class descriptions of both natural forests and rubber plantation. The threshold that could separate natural forests and rubber plantations to it was calculated threshold from the separability analysis of candidate vegetation indices (NDVI, EVI, LSWI, and SWIR1), and their threshold from the analysis shown in 3.1. While for extended object-based phenology approach, we used nearest neighbor classifier to separate natural forests and rubber plantations, please see the following for details.

2.4.3.Extended object-based phenology approach

For the extended object-based phenology approach, we used Nearest Neighbor classifier based on optimized composition of different features (the three VIs and other VIs based on these three VIs, see later in this part) that most suitable for separating classes to classify natural forests and rubber plantations. The extended object-based phenology approach adopted the same segmentation and hierarchy classes as with the object-based phenology approach above being also applied at two levels, with the first level classification being same as in the object-based phenology approach above. The difference between these two object-based approaches lies in the second level classification where the extended object-based phenology approach used the Nearest Neighbor classifier of eCognition (Version 8.0, Trimble) to determine the best combination of features to differentiate rubber plantations and natural forests. The object-based phenology approach used the decision tree classifier to separate natural forests and rubber plantations as that of pixel-based phenology approaches. In other words, to classify natural forests and rubber plantations, the extended object-based phenology approach used sample-based Nearest Neighbor classifier (Table 2), while the object-based phenology approach used expert knowledge based decision tree classifier. Both the object-based and extended object-based phenology approaches used membership function in the second level to classify waterbodies and other land use types (Table 2).Additionally, more vegetation indices of both defoliation and foliation stages were developed and put into the Nearest Neighbor classifier. We used the Nearest Neighbor classifier of eCognition (Version 8.0, Trimble) to classify rubber plantations and natural forests. Firstly, 50 samples that are representatives for each class were manually selected from the image objects. Then we trained Nearest Neighbor classification algorithm to differentiate each class by mathematically calculating the best combination of features (the three vegetation indices and SWIR1 and the developed indices based on the three vegetation indices and SWIR1) in the feature space with Feature Space Optimization function of Nearest Neighbor classification algorithm. After this process, the image objects were assigned to each class by calculating the closest image object with selected features from above calculation. We developed several additional indices based on the three VIs (NDVI, EVI, and LSWI)and SWIR1 used for the extended object-based phenology approach, for NDVI: $NDVI_{defoliate}$-$NDVI_{refoliate}$, $NDVI_{defoliate}$+$NDVI_{refoliate}$, $NDVI_{defoliate}$/$NDVI_{refoliate}$, NDVIratio= ($NDVI_{defoliate}$-$NDVI_{refoliate}$)/ ($NDVI_{defoliate}$+$NDVI_{refoliate}$), and also similar calculations for EVI, LSWI, and SWIR1.

2.5. Validation and comparison

The resultant thematic map of natural forests, rubber plantations and other types of land cover at 30 m spatial resolution was evaluated by using a confusion matrix based on the ROIs for validation (Table 3). The ROIs for validation were collected from previous ground truth

data and from high geometric precision and fine spatial resolution Google Earth imagery. For the accuracy assessment, ground truth data of rubber plantation older than ten years were selected, yielding thirty ROIs (30 vs. 50 for total rubber ROIs) of rubber plantations. All the sixteen ROIs of natural forests were collected from Google Earth.

A total of 84 polygon ROIs (~ 21,500 pixels) were created from Google Earth to conduct accuracy assessments, including 16 natural forests ROIs (9,189 pixels), 50 rubber ROIs (3,469 pixels), and 18 ROIs (8,656 pixels) for other types of land cover. The ROIs were randomly and widely distributed in the study area. All the resultant maps were assessed using these ROIs.

Table 3. Accuracy assessment of the land cover classification map of Xishuangbannabased on Landsat 7 ETM+ images using the pixel-based phenology approach, the object-based phenology approach, and the extended object-based phenology approach.

The pixel-based phenology approach	Classes	Ground-truth (Pixels) Rubber	Others	Total classified pixels	User's accuracy
Classified results	Rubber	2835	296	3131	90.5%
	Others	663	17551	18214	96.4%
Total ground truth pixels		3498	17847	21345	
Producer's accuracy		81.0%	98.3%		
Overall accuracy		95.5%			
Kappa coefficient		0.83			

3. Results

3.1. Rubber plantation phenology characteristics in Xishuangbanna

The seasonal dynamics of MODIS derived NDVI of rubber plantations and natural forests showed that rubber plantations only have a distinct different phenology compared to natural forests during the defoliation and (re)foliation periods (Fig.2). Hence, we selected eleven Landsat TM/ETM+ images from 2002-2003, covering the corresponding defoliation/(re)foliation time span. Landsat images and results from field observations confirmed that during the dry season, rubber trees defoliate substantially in early January to early February; thereafter, rubber trees underwent rapid (re)foliation and canopy recovery from February to early March (Figs. 4 & 6). However, during the rainy season (May to October) results from field observation and satellite images suggested that rubber plantations had similar NDVI levels to those of natural forests during the rainy season (Figs. 2& 4).

Preprints (www.preprints.org) | NOT PEER-REVIEWED | Posted: 6 August 2016 doi:10.20944/preprints201608.0069.v1

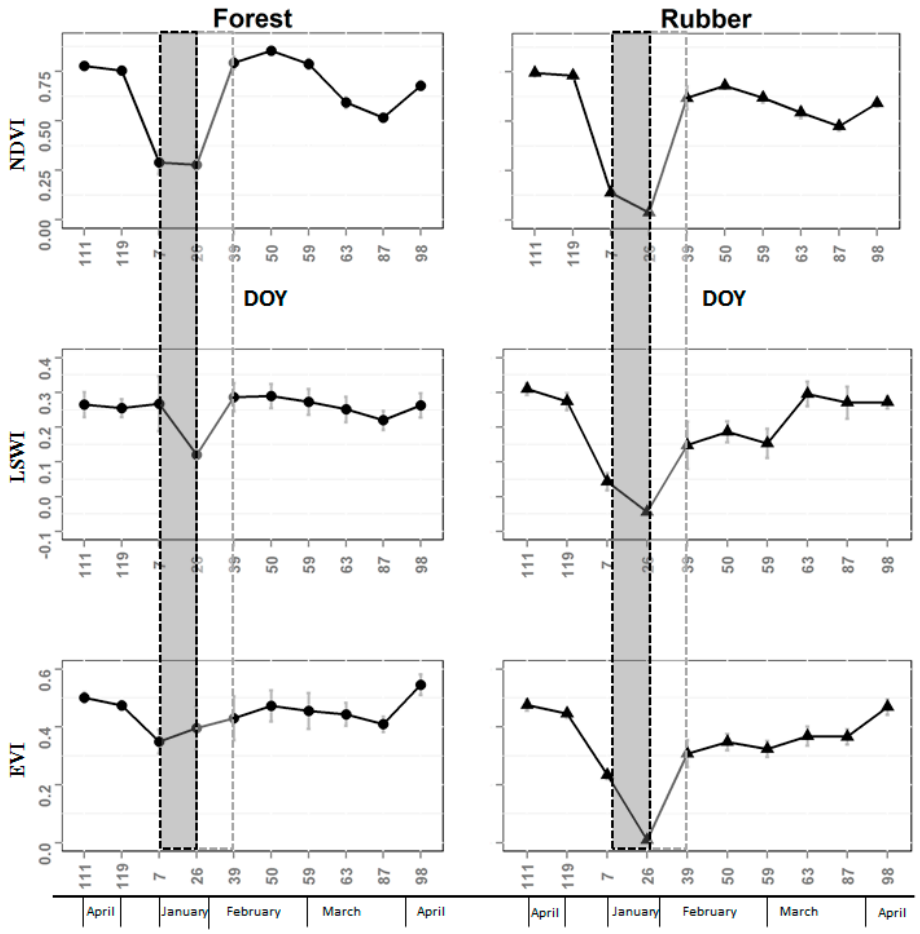

Fig.6. Temporal profiles of time series Landsat NDVI, EVI, and LSWI reflectance for natural forests, and rubber plantations. Twelve points of interest (POIs) were extracted for rubber plantations and 13 POIs for natural forests. The points and error bars show their average and standard deviation (SD) values. Rubber plantations and natural forests are evidently different in two typical phenology phases: defoliation (the gray long and narrow boxes) and foliation (the white long and narrow boxes).

The Landsat derived vegetation indices showed that rubber plantations had lower NIR, NDVI and EVI values than natural forests during the defoliation stage, and had higher NIR, NDVI and EVI values than natural forests in the foliation stage(Fig. 7), which suggests that rubber plantations can be separated from natural forests based on different phenological characteristics during these two stages. A more detailed spectral analysis suggested that during defoliation stage, SWIR1, SWIR2, NDVI, LSWI, and EVI showed a higher ability to separate rubber plantations from natural forests than others(Fig. 7). SWIR1 (0.263±0.039), SWIR2 (0.169±0.026) of rubber plantations were higher at maximum defoliation than that of natural forests, with 0.123±0.030 and 0.052±0.013, respectively. Additionally, NDVI(0.467±0.023), LSWI (-0.086±0.031), and EVI (0.276±0.026) of rubber plantations were much lower than the natural forests, 0.783±0.024, 0.362±0.043 and 0.460±0.087, respectively(Fig. 7). During the (re)foliation stage, although rubber plantations and natural forests have similar spectral values in the other six bands, NIR, SWIR1, and EVI showed good ability to separate rubber plantations (0.357±0.033, 0.189±0.020, and0.627±0.053, respectively) from natural forests (0.279±0.024, 0.131±0.013, and0.491±0.039, respectively) (Fig. 7).Hence,

 doi:10.20944/preprints201608.0069.v1

both the defoliation and foliation stages showed a high potential to identify and separate rubber plantations from natural forests. In particular, SWIR1 and EVI showed performed better during both defoliation and foliation stages, than the other indices or spectral bands(Fig. 7). Therefore, we usedSWIR1>=0.156 and EVI(defoliation) <= 0.338∪EVI (foliation) >= 0.566 for the object-based phenology approach, but all the derived indices (NDVI, LSWI, SWIR1, and EVI) for the extended object-based phenology approach for rubber plantation and natural forest classification.

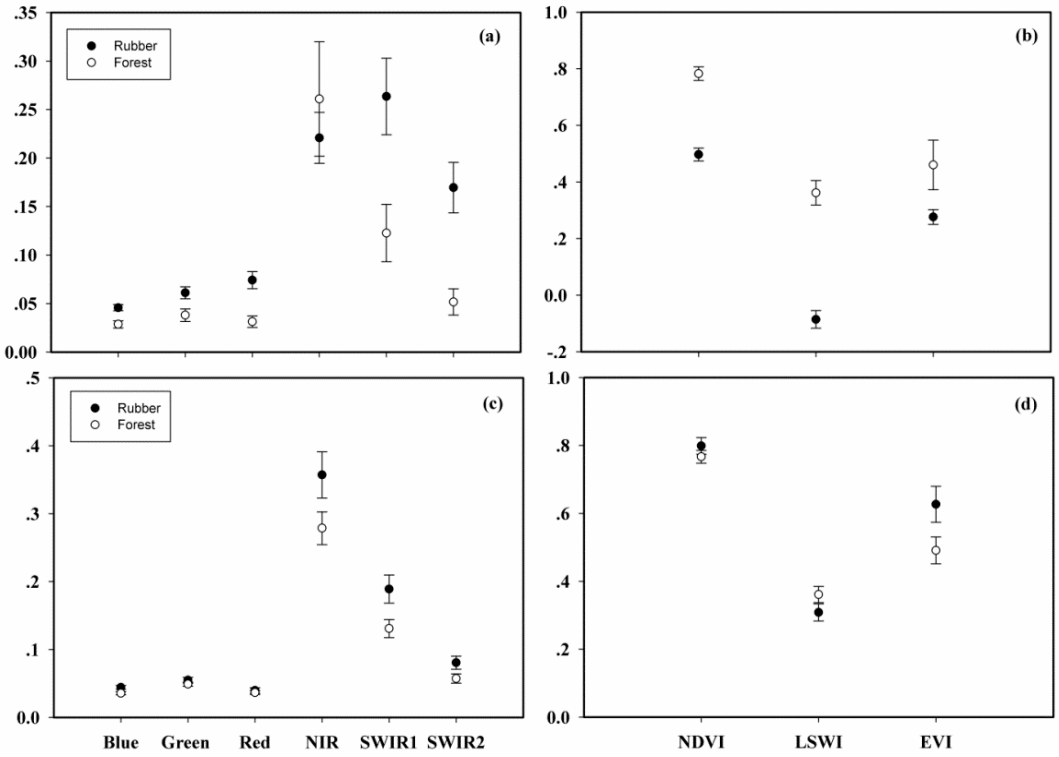

Fig.7. Signature analysis of the reflectance of the six spectral bands (Blue, Green, Red, NIR, SWIR1, and SWIR2) for rubber plantations and natural forests based on (a) Landsat 7 ETM+ images of February 19th, 2003 & (c) April 21st, 2002; and signature analysis of the reflectance of the vegetation indices (NDVI, EVI and LSWI) for rubber plantations and natural forests based on (b) Landsat 7 ETM+ images of February 19th, 2003 and (d) April 21st, 2002. Rubber plantations and natural forests have distinctive SWIR1 and EVI values.

3.2. Rubber plantation map in Xishuangbanna and accuracy assessment

Two rubber plantation maps were finally generated using the two object-based phenology approaches. The rubber plantation area in Xishuangbanna was estimated at 1342.7km^2 according to the object-based phenology approach, which was lower than the estimate of 1526.2 km^2 from previous research of by Xu, *et al.* [14] that of the extended object-based phenology approach was 1866.0 km^2 (Fig. 8).

The extended object-based phenology approach achieved an overall accuracy of 97.4%, which was higher than that of the object-based phenology approach (96.4%) (Table3). The extended object-based phenology approach discriminated better between natural forests and rubber plantations, and the producer's accuracy (higher values indicate lower commission error) was higher than that of the object-based phenology approach, while the user's accuracy (higher values indicate lower omission error) was lower than that of the object-based

Preprints (www.preprints.org) | NOT PEER-REVIEWED | Posted: 6 August 2016 doi:10.20944/preprints201608.0069.v1

phenology approach. The object-based phenology approach using only SWIR1 and EVI thresholds to differentiate natural forests and rubber plantation showed lower producer's accuracy (95.7%) of rubber plantations compared to that of the extended object-based phenology approach (99.4%) (Table3), which is higher than that observed by Senf, *et al.* [23] (63.6% with a pixel based SWIR and EVI model), which might have been caused by their coarser resolution (250 m (their research) vs. 30 m (our research)) (Table 3). However the producer's accuracy for rubber plantations identified via the object-based phenology approach was higher than that of pixel-based phenology approach (81.0%) (Table3). The resulting non-forest and natural forest/rubber plantation map using the extended object-based phenology approach achieved a high accuracy according to the confusion matrix by using the ground truth ROIs. The overall accuracy of the extended object-based phenology approach was 97.4% and the Kappa coefficient was 0.96 (Table 3). The interpretation accuracy of rubber plantation was a. 90% for both the user's and producer's accuracy, and the other land cover types i.e. natural forests and others had user's and producer's accuracies of higher than 96%.

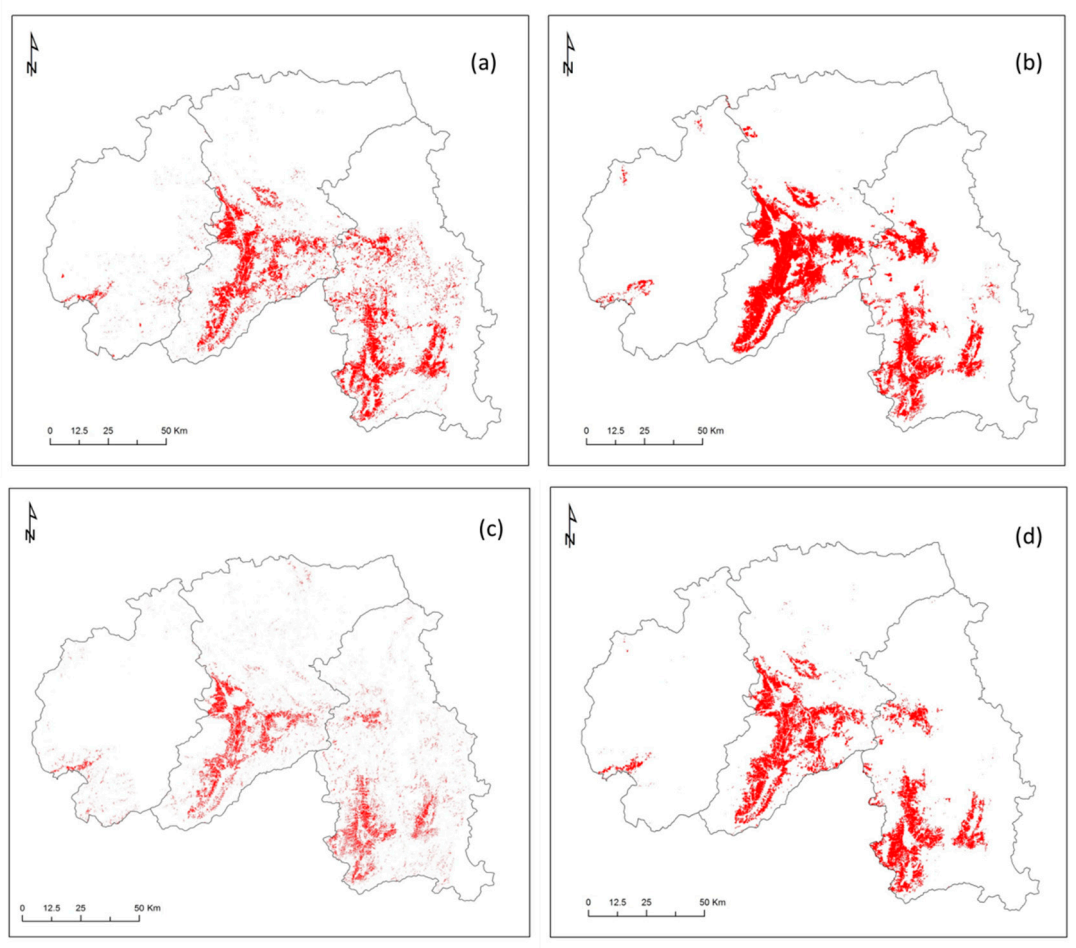

Fig.8. The resultant rubber plantation map derived by the object-based phenology approach (a), the extended object-based phenology approach (b), the pixel-based phenology approach (c),and the compared rubber plantation map developed by Xu, *et al.* [14] (d).

The extended object-based phenology approach showed the lowest omission error compared to the other two approaches, however, it showed the highest commission error (Table 3).The highest omission error of the pixel-based phenology approach might have been

Preprints (www.preprints.org) | NOT PEER-REVIEWED | Posted: 6 August 2016 doi:10.20944/preprints201608.0069.v1

caused by rubber ages, topography, and different defoliation features of the rubber plantation during the defoliation phase (Fig. 9).

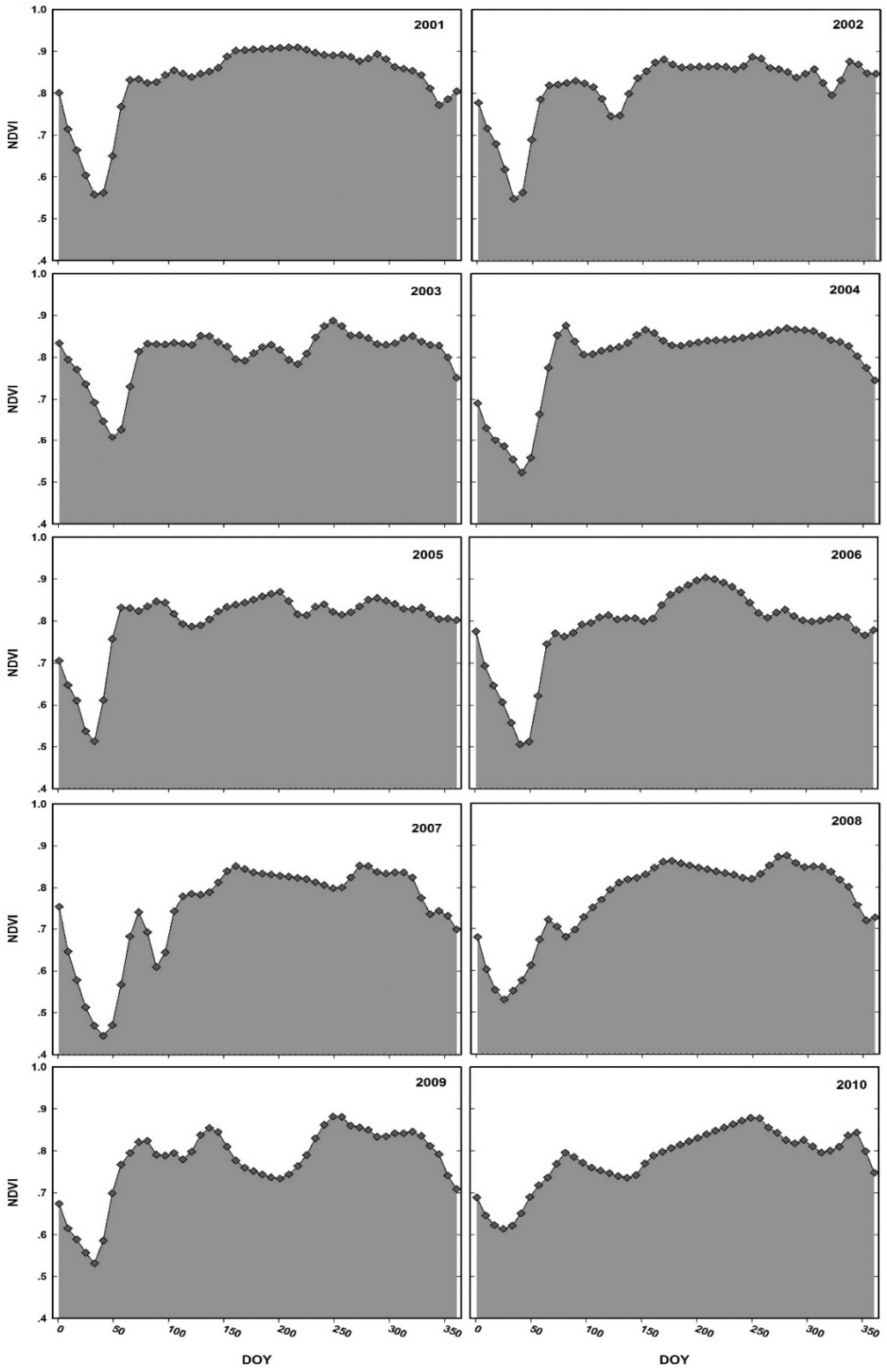

Fig.9 Temporal changes of NDVI in Xishuangbanna in 2001-2010.

 doi:10.20944/preprints201608.0069.v1

4. Discussion

4.1. Performance of the phenology-based approach for rubber plantation

The results from this study showed that deciduous rubber plantations can be identified and mapped rapidly and effectively with images acquired during designated phenological phases (defoliation or foliation). The distinct difference in phenology between rubber plantations and natural forests in the study area occurred during two specific phenological phases: the defoliation and foliation stages of rubber plantations (Fig.6), which confirmed observation by other researchers [19,22,42,48,49]and which was proven by our MODIS results (Fig.2). These two phenological phases are quite useful for mapping rubber plantations in tropical China and have been applied to delineate rubber plantations from natural forests[19,23].

Previous non-phenology related studies have also realized the defoliation phase for separating natural forests and rubber plantations in Xishuangbanna by specifically selecting images from the dry season[7,10]. As pointed out recently in other studies [19,42], our research also indicated that both defoliation and foliation phases are important phenology-based phases for identifying and mapping rubber plantation. However, most studies used only one image either from the defoliation or foliation phase to delineate rubber plantations from natural forests[19,42,48,49]. For the proposed approach in this research, two phases of images are required to effectively map rubber plantations and natural forests by selecting and using images from the defoliation and foliation phases; specifically, one from these two phenological phases and the other one from the growth stage. Different phenological features are represented by different VIs for rubber plantations and natural forests: 1) during the defoliation phase (Early January to early February) rubber plantations have a canopy with little or no green leaves (Fig. 4) and low NDVI/EVI/LSWI values, while sampled natural forests exhibit only slight changes in canopy coverage with high VI values (Fig. 6). This is true for tropical evergreen forests, while the deciduous natural forests, from the observed site evidence, shed leaves gradually from January to April and then refoliate from April to June[50]; 2) during the foliation phase (February to early of March), rubber trees have rapid (re)foliation (new leaf emergence) and canopy recovery (Fig. 4), which results in high reflectance in near infrared bands (NIR), and increasing of NDVI/EVI/LSWI values. By comparison, natural forests have relatively lower NIR values and comparatively smaller change while maintaining high NDVI/EVI/LSWI values (Fig. 6).

This study emphasizes the utility of phenology-based image selection for deciduous rubber plantation classification. The phenology-based images were categorized into three phases: defoliation, foliation, and growth. Cloud cover in this tropical region was an obstacle to acquire more required sufficient fine resolution images (e.g. Landsat, HJ (a Chinese environmental satellite), SPOT, and RapidEye), so images during the dry season were selected in previous studies[7,20]. Both defoliation and foliation phases appeared during the dry season. During the rainy season (from May to October), it is hard to find high quality images due to cloud cover. However, it is possible to get the necessary images from November to December, which is a cool dry season in Xishuangbanna and rubber trees are not shedding leaves[29,51]. The approach proposed in this study would provide solutions not only for the coarse resolution MODIS(as we use 30m resolution Landsat images) but also for similar spectral features of rubber plantation and other forests in land use classification by Landsat. This phenology-based image selection and Landsat-based phenological analysis provide high resolution information of seasonal vegetation changes and finer spatial information than MODIS at 250m or 500m resolutions and often mixes other types of land cover. Previous research in Hainan Province, China also found that Landsat could capture leaf shedding during the defoliation stage and a rapid recovery of rubber trees during the foliation stage for intra-annual phenology characterization at 30m resolution[19]. Similarly, in this study, e.g.

NDVI, LSWI, and EVI showed an evident decrease during the defoliation stage of rubber plantations (early January to early February), LSWI, in particular, can reach values below 0 while those of natural forests always remain above 0. Furthermore, LSWI values of natural forests were above 0 at both dates. This finding is consistent with Xiao, *et al.* [37] and Kou, *et al.* [42], who found that LSWI values of natural evergreen forests were always higher than 0 over the whole year while deciduous forest showed a period of LSWI below 0. The study indicated the importance of LSWI for mapping rubber plantations during the defoliation phase. The SWIR and EVI proved best able to discriminate rubber plantation from natural forests in both the defoliation and foliation phases.

The phenology based approach led to a comparatively higher accuracy and efficiency mapping of rubber plantations and other forest types than non-phenology based approaches[7,12,20]. A phenology-based land use/land cover mapping has also proved effective for rice paddy extraction[52]. The phenology-based approach in this research led to a higher resolution rubber plantation map by using Landsat images during a critical phenological phase (e.g., at the end of March in this study). The finer spatial resolution Landsat imagery provides more spatial details about the extent and spatial configuration of rubber plantations than MODIS imagery[20,23], and it is more appropriate for a highly fragmented hilly rubber developing region as Xishuangbanna [23,53].

4.2 Comparison of object- vs pixel-based approaches in phenology-based mapping

This research suggests that the object based approaches were able to improve the accuracy of rubber mapping better than pixel-based phenology approaches, e.g. achieving higher overall accuracy (96.4%, and 97.4% respectively, Table 3) compared to the 73.5% reported by Senf, *et al.* [23] and the92% of Dong, *et al.* [19].The object-based phenology approach was overall sufficient to extract rubber plantation and natural forests, but higher accuracy was achieved using more vegetation based spectral variable in the extended object-based phenology approach although this came with a commission error penalty. Therefore, using the object-based phenology approach has its advantages in: 1) reducing redundancies and multi-collinearity when processing the classification;2) making it much easier to track the changes of natural forests and rubber plantations; and3) facilitating the transferability of the approach to other regions. The higher accuracy of object-based results might attribute to the identical characteristic image texture caused by land form and landscape terracing when planting [7] which was demonstrated by finer spatial resolution imageries in Google Earth and clear geographical distribution patterns[18] (see Fig.10).

Preprints (www.preprints.org) | NOT PEER-REVIEWED | Posted: 6 August 2016 doi:10.20944/preprints201608.0069.v1

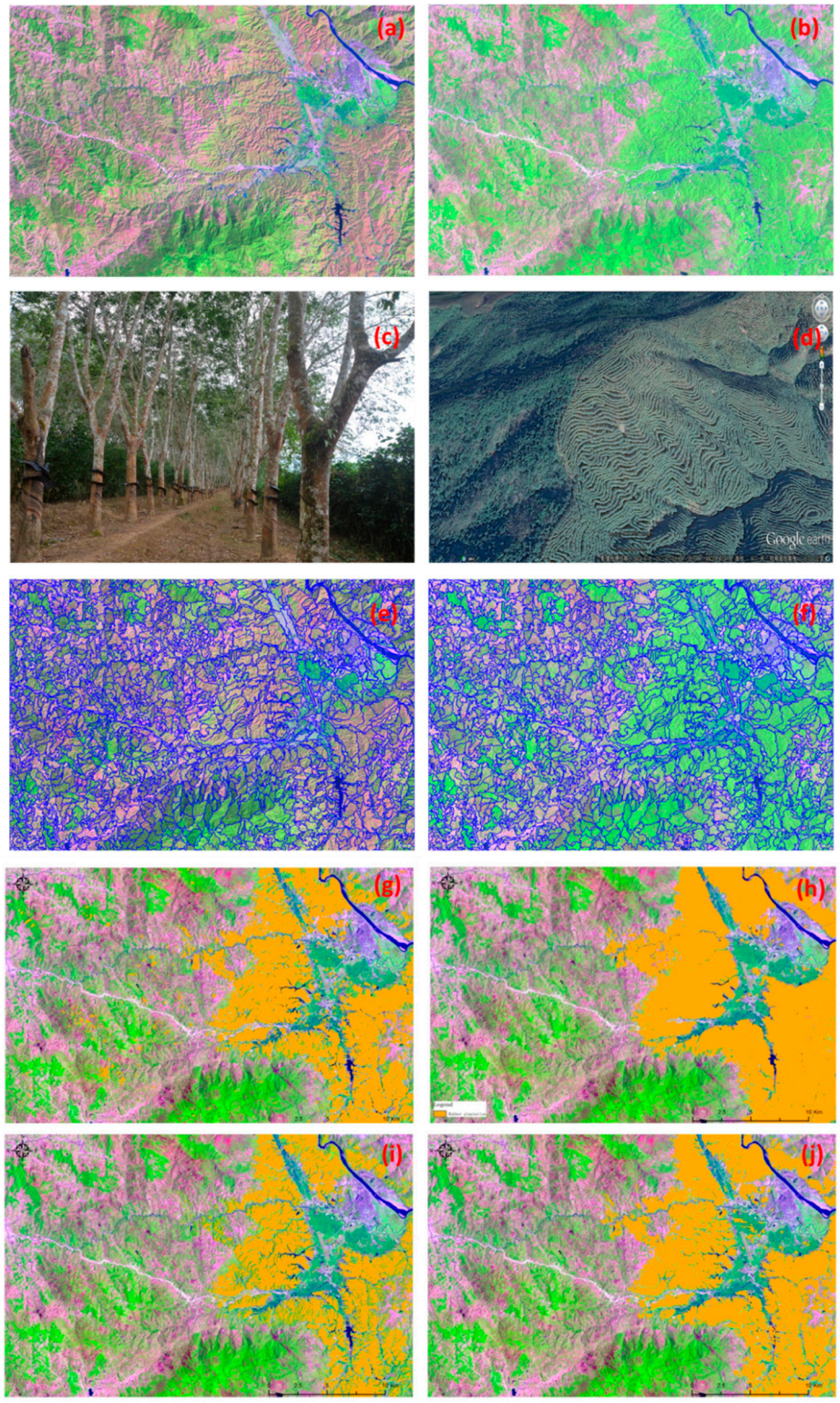

Fig.10. False color composition map (R/G/B = Band 5/4/3) of Landsat images (a) —February 19th, 2003; (b) —April 8th, 2002;(c) photo taken in the field; (d) image from finer resolution images in Google Earth, with natural forests on the left and rubber plantations on the right; (e)segmentation of image (a); (f) segmentation of image (b); (g) classification of object-based phenology approach; (h) classification of extended object-based phenology approach; (i) classification of pixel-based phenology approach; and (j) thematic map of Xu, *et al.* [14].

 doi:10.20944/preprints201608.0069.v1

Combining PALSAR and Landsat images to map rubber plantations and natural forests [19,42] also showed its advantages; however, some uncertainties were also brought up when using the PALSAR (topographic factors and stand age factors affected the forest mask extracted by PALSAR [42]) in highly mountainous region, which could also be found in Table 3 with a lower producer's accuracy of rubber plantations identified via the pixel-based approach. However, the object-based approach can overcome this problem by its hierarchical classification, which is optimized for applying complex class hierarchies to the entire image object level (eCognition, Version 8.0, Trimble). By using this hierarchical classification, the parent vegetation class was extracted, and then two child classes—rubber plantations and natural forests were extracted based on their parent class—vegetation class. This makes good use of Landsat information rather than relying on other sensors to extract forest layer[19,48,49].

4.3 Uncertainty analysis for rubber plantation mapping

We identified a distinctive defoliation phase of rubber trees from early January to early February, and a (re)foliation phase from middle February to early March in Xishuangbanna, which agrees with reports of other researchers based on site-based observations(Jia, 2006; Song et al., 2014) and also our own investigations (Fig. 4). However, our results are not fully aligned in time with those of Guardiola-Claramonte et al. (2008), who found defoliation from late February to late March, and refoliation during April in Nam Ken, Xishuangbanna, which is quite consistent with observations in Hainan[19].

Rubber trees in Xishuangbanna show clearer defoliation and foliation phases than those of Hainan[19], and rubber trees in Xishuangbanna start each phase earlier than in Hainan. This is consistent with comments by Dong, *et al.* [19], who mentioned that there could be temporal inconsistencies for the phenology of rubber trees in different latitudes compared to their findings. However, we not only found inconsistency of the phenological phases compared to that of Hainan but also the inconsistencies in different years (Fig. 9). We find there is a difference of 24 days between the starts of the foliation phase in different years (Fig. 9), which alter the required data acquisitions for rubber plantation mapping. The changing phenological phase in different years causes a lower effectiveness of the pixel-based phenology approach for rubber plantation mapping. Additionally, there are phenological phase inconsistencies in different sites of the same region in one year (Fig. S1), which could be the reason for the limitations of the pixel-based phenology approach in mountainous and fragmented areas. The inconsistency might relate to climate, latitude, elevation, rubber ages and varieties[54], the variations of which could lead to variations in phenology. Therefore, it is necessary to check the defoliation and foliation phases (using MODIS) before acquiring data for rubber plantation mapping. In the future, a systematic investigation and study of rubber trees at local regional level will benefit rubber plantation mapping and rubber plantation phenological phase projection under climate changes.

The complicated meaning of parameter and the subjective or experience-based parameter selection in eCognition [44,46,55], especially for scale parameter, could be a limitation of parameter selection in different regions. In eCognition, a post-evaluation-based approach is often applied in multi-resolution segmentation, which is difficult to quantitatively achieve the most suitable parameters in image segmentation even with repetitious trial processing [46,55]. To reduce the subjectiveness and to quantify the parameters during segmentation, researches have adopted statistics-based or spatial statistics-based procedures (a focal mean, local variance, estimation of scale parameter tool, or semi-variagram related methods) to select the optimized parameters [55-59]. However, most of this research is based on the post-evaluation-based approach[55]. The pre-estimation method is found to be a solution to enhance the efficiency and quantity of the object-based classification approach[55]. Future research for automatic parameter selection by a pre-estimation might help to enlarge the

application of the object-based phenology approach in rubber development regions, while a more detailed research on this is beyond the scope of this study.

4.4 Implication on extensive application

For the application of the phenology based and in particular the object-based approaches (the two object-based approaches in this research) in a new region, it is suggested to delineate the changes of rubber plantation and other forest types by MODIS first. With the help of MODIS's high temporal resolution, a detailed temporal seasonal dynamic of rubber plantations and natural forests patterns could be recorded and hence the temporal window of distinct phenological phases identified. Once the temporal window was identified and the defoliation and foliation phases of rubber are defined, two higher resolution optical images from different phenological phases are sufficient to map the distribution of rubber plantations and natural forests at regional scale. We also found that Google Earth could be used to identify the two phases (Fig. S2), which is consistent with what we observed at the local site (Fig. 4). This will simplify and improve the mapping efficiency of regional rubber plantations and natural forests. These approaches could also be applied to other land uses (e.g. paddy land) with clearly distinct phenological features. Another potential solution is to find the bioclimatic factor related to defoliation and foliation of rubber plantations (e.g. air temperature has been used by Dong, *et al.* [52] to identify phenology timing of paddies, which was then applied for phenology-based image selection), and then use the results to identify the phenological stages of rubber plantations in southeast Asia which will be used for image selection later. This shows great potentials to improve the efficiency and accuracy of rubber plantation mapping in the Southeast Asia.

The object-based approaches in this research might also be able to improve the accuracy of paddy lands over to the pixel-based phenology approach used by Dong, *et al.* [52]. It shows great potential to apply these approaches to other regions and other land types. The approach in this research could also being used with other optical satellite images (e.g. HJ (30 m)), or higher resolution satellite images (e.g. RapidEye (5 m), SPOT (5 m), GeoEye (0.5 m)) to facilitate the mapping of rubber plantations and other forest types.

5. Conclusions

In this research, a new object-based phenology approach for the mapping natural forests and rubber plantations in Xishuangbanna was successfully developed, by combining phenological metrics derived from time series Landsat with object-based approaches. Our study revealed the advantages of the object-based strategy in comparison to the pixel-based strategy when using phenological metrics in discriminating rubber plantations and natural forests. Based on the above results, we can draw two conclusions. First, the phenology-based approach is effective and robust in rubber plantation mapping in mountainous Xishuangbanna, and Landsat can capture the phenological features of rubber plantations. According to the phenological features of rubber plantations, three distinct stages were identified: the defoliation, foliation, and growth stages. Both defoliation and foliation could distinguish rubber plantation from natural forests. Second, the object-based phenology approaches were better able to identify rubber plantations in highly fragmented regions than the pixel-based phenology approach. Given the increasing temporal resolution of Landsat OLI imagery, this object-based phenology approach would be adopted to map rubber plantations annually at a 30 m resolution in the future. However, an extensive application of the approach needs consider the phenology variation of rubber plantations in different regions. Moreover, the influence of site conditions (e.g. slopes, aspect, and elevation), climate, and rubber age and varieties on the method application should be examined for further improvement in the accuracy of phenology-based regional mapping.

Supplementary Materials: The following are available online at www.mdpi.com/link, Figure S1: Photo taken on the same day in Menglun Township. A) Rubber trees still with green leaves. B) Rubber plantation already entered into late phase of leaf coloring and start of litterfall., Figure S2: Observed temporal changes of rubber plantation in Xishuangbanna by Google Earth with three satellite images (upper: November 6th, 2013; Middle: February 2nd, 2014; down: March 18th, 2014). Table S1: Landsat mission.

Acknowledgments: This work is funded in part by the National Natural Science Foundation of China (No.31300403, 31400493), the China Postdoctoral Science Foundation (No. 2013M540722), and the NASA Land Use and Land Cover Change program (No. NNX14AD78G). All the cost related to this research for publishing in open access journal will be covered by the National Natural Science Foundation of China (No.31300403). This work was additionally supported by a visiting scientists grant to Deli Zhai from the Food Security Center (FSC) visiting postdoctoral researchers program that is supported by the German Academic Exchange Service (DAAD) with funds of the Federal Ministry of Economic Cooperation and Development (BMZ) of Germany. The research is part of the BMZ/GIZ "Green Rubber" (No. 13.1432.7-001.00) and 'SURUMER' (No. 01LL0919A) projects with the financial support of the Federal Ministry for Economic Cooperation and Development, Germany. This research is also part of the CGIAR Research Program 6: Forests, Trees, and Agroforestry. The authors appreciated the help from Chen Hua-Fang from the World Agroforestry Centre's East and Central Asia regional program and Dr. Sergey Blagodatsky from the University of Hohenheim for their useful comments and suggestions on rubber plantation distribution. We would like to thank Dr. Dai Zhi-Cong from Jiangsu University for helping with the figures.

Author Contributions: Deli Zhai, Jinwei Dong, Jianchu Xu, and Xiangming Xiao designed this study. Deli Zhai conducted the data processing and manuscript writing. Jinwei Dong supported the data preparation, technical support and analysis. Georg Cadisch, Mingcheng Wang, and Weili Kou contributed to the MODIS and other related data preparation, processing and manuscript editing. All the authors contributed on the interpretation of results and manuscript revision.

Conflicts of Interest: The authors declare no conflict of interest.

References

1. Koh, L.P.; Wilcove, D.S. Is oil palm agriculture really destroying tropical biodiversity? *Conservation Letters* **2008**, *1*, 60-64.
2. Ziegler, A.D.; Fox, J.M.; Xu, J.C. The rubber juggernaut. *Science* **2009**, *324*, 1024-1025.
3. FAO. Global forest resources assessment 2010. *FAO Forestry Paper* **2010**.
4. Li, Z.; Fox, J.M. Mapping rubber tree growth in mainland southeast asia using time-series modis 250 m ndvi and statistical data. *Applied Geography* **2012**, *32*, 420-432.
5. Prachaya, J. Rubber economist quarterly report. *London and Bangkok.* **2009**.
6. Fox, J.; Vogler, J.B. Land-use and land-cover change in montane mainland southeast asia. *Environmental Management* **2005**, *36*, 394-403.
7. Zhai, D.-L.; Cannon, C.H.; Slik, J.W.F.; Zhang, C.-P.; Dai, Z.-C. Rubber and pulp plantations represent a double threat to hainan's natural tropical forests. *Journal of Environmental Management* **2012**, *96*, 64-73.
8. Xu, J.C.; Ma, E.T.; Tashi, D.; Fu, Y.S.; Lu, Z.; Melick, D. Integrating sacred knowledge for conservation: Cultures and landscapes in southwest china. *Ecology and Society* **2005**, *10*.
9. Sturgeon, J.C. Cross-border rubber cultivation between china and laos: Regionalization by akha and tai rubber farmers. *Singapore Journal of Tropical Geography.* **2013**, *34*, 70-85.
10. Fu, Y.; Chen, J.; Guo, H.; Hu, H.; Chen, A.; Cui, J. Agrobiodiversity loss and livelihood vulnerability as a consequence of converting from subsistence farming systems to commercial plantation-dominated systems in xishuangbanna, yunnan, china: A household level analysis. *Land Degradation & Development* **2010**, *21*, 274-284.

11. Guardiola-Claramonte, M.; Troch, P.A.; Ziegler, A.D.; Giambelluca, T.W.; Durcik, M.; Vogler, J.B.; Nullet, M.A. Hydrologic effects of the expansion of rubber (hevea brasiliensis) in a tropical catchment. *Ecohydrology* **2010**, *3*, 306-314.
12. Li, H.M.; Ma, Y.X.; Aide, T.M.; Liu, W.J. Past, present and future land-use in xishuangbanna, china and the implications for carbon dynamics. *Forest Ecology and Management* **2008**, *255*, 16-24.
13. Grogan, K.; Pflugmacher, D.; Hostert, P.; Kennedy, R.; Fensholt, R. Cross-border forest disturbance and the role of natural rubber in mainland southeast asia using annual landsat time series. *Remote Sensing of Environment* **2015**, In press.
14. Xu, J.; Grumbine, R.E.; Beckshafer, P. Landscape transformation through the use of ecological and socioeconomic indicators in xishuangbanna, southwest china, mekong region. *Ecological Indicators* **2014**, *36*, 749-756.
15. Qiu, J. Where the rubber meets the garden. *Nature* **2009**, *457*, 246-247.
16. Li, H.M.; Aide, T.M.; Ma, Y.X.; Liu, W.J.; Cao, M. Demand for rubber is causing the loss of high diversity rain forest in sw china. *Biodiversity and Conservation* **2007**, *16*, 1731-1745.
17. Liu, X.; Feng, Z.; Jiang, L. Application of decision tree classification to rubber plantations extraction with remote sensing. *Transactions of the Chinese Society of Agricultural Engineering* **2013**, *29*, 163-172+365.
18. Liu, X.; Feng, Z.; Jiang, L.; Zhang, J. Rubber plantations in xishuangbanna: Remote sensing identification and digital mapping. *Resources Science* **2012**, *34*, 1769-1780.
19. Dong, J.; Xiao, X.; Chen, B.; Torbick, N.; Jin, C.; Zhang, G.; Biradar, C. Mapping deciduous rubber plantations through integration of palsar and multi-temporal landsat imagery. *Remote Sensing of Environment* **2013**, *134*, 392-402.
20. Li, Z.; Fox, J.M. Integrating mahalanobis typicalities with a neural network for rubber distribution mapping. *Remote Sensing Letters* **2011**, *2*, 157-166.
21. Chen, H.; Chen, X.; Chen, Z.; Zhu, N.; Tao, Z. A primary study on rubber acreage estimation from modis-based information in hainan. *Chinese Journal of Tropical Crops* **2010**, 1181-1185.
22. Dong, J.; Xiao, X.; Sheldon, S.; Biradar, C.; Duong, N.D.; Hazarika, M. A comparison of forest cover maps in mainland southeast asia from multiple sources: Palsar, meris, modis and fra. *Remote Sensing of Environment* **2012**, *127*, 60-73.
23. Senf, C.; Pflugmacher, D.; van der Linden, S.; Hostert, P. Mapping rubber plantations and natural forests in xishuangbanna (southwest china) using multi-spectral phenological metrics from modis time series. *Remote Sensing* **2013**, *5*, 2795-2812.
24. Cheng, G.; Han, J.; Guo, L.; Liu, Z.; Bu, S.; Ren, J. Effective and efficient midlevel visual elements-oriented land-use classification using vhr remote sensing images. *Ieee Transactions on Geoscience and Remote Sensing* **2015**, *53*, 4238-4249.
25. Cheng, G.; Guo, L.; Zhao, T.; Han, J.; Li, H.; Fang, J. Automatic landslide detection from remote-sensing imagery using a scene classification method based on bovw and plsa. *International Journal of Remote Sensing* **2013**, *34*, 45-59.
26. Cheng, G.; Han, J.; Zhou, P.; Guo, L. Multi-class geospatial object detection and geographic image classification based on collection of part detectors. *ISPRS Journal of Photogrammetry and Remote Sensing* **2014**, *98*, 119-132.
27. Mittermeier, R.A.; P. Robles Gil; M. Hoffman; J. Pilgrim; T. Brooks; C. G. Mittermeier; J. Lamoreux; Fonseca, a.G.A.B.d. *Hotspots revisited: Earth's biologically richest and most endangered terrestrial ecoregions*. lavoisier.fr CEMEX, Mexico., 2005.
28. Zhu, H.; Cao, M.; Hu, H.B. Geological history, flora, and vegetation of xishuangbanna, southern yunnan, china. *Biotropica* **2006**, *38*, 310-317.

29. Liu, W.J.; Liu, W.Y.; Li, P.J.; Gao, L.; Shen, Y.X.; Wang, P.Y.; Zhang, Y.P.; Li, H.M. Using stable isotopes to determine sources of fog drip in a tropical seasonal rain forest of xishuangbanna, sw china. *Agricultural and Forest Meteorology* **2007**, *143*, 80-91.
30. Song, Q.; Lin, H.; Zhang, Y.; Tan, Z.; Zhao, J.; Zhao, J.; Zhang, X.; Zhou, W.; Yu, L.; Yang, L.; Yu, G.; Sun, X. The effect of drought stress on self-organisation in a seasonal tropical rainforest. *Ecological Modelling* **2013**, *265*, 136-139.
31. Xu, J. The political, social, and ecological transformation of a landscape - the case of rubber in xishuangbanna, china. *Mountain Research and Development* **2006**, *26*, 254-262.
32. Guardiola-Claramonte, M.; Troch, P.A.; Ziegler, A.D.; Giambelluca, T.W.; Vogler, J.B.; Nullet, M.A. Local hydrologic effects of introducing non-native vegetation in a tropical catchment. *Ecohydrology* **2008**, *1*, 13-22.
33. Roy, D.P.; Wulder, M.A.; Loveland, T.R.; C.E, W.; Allen, R.G.; Anderson, M.C.; Helder, D.; Irons, J.R.; Johnson, D.M.; Kennedy, R.; Scambos, T.A.; Schaaf, C.B.; Schott, J.R.; Sheng, Y.; Vermote, E.F.; Belward, A.S.; Bindschadler, R.; Cohen, W.B.; Gao, F.; Hipple, J.D.; Hostert, P.; Huntington, J.; Justice, C.O.; Kilic, A.; Kovalskyy, V.; Lee, Z.P.; Lymburner, L.; Masek, J.G.; McCorkel, J.; Shuai, Y.; Trezza, R.; Vogelmann, J.; Wynne, R.H.; Zhu, Z. Landsat-8: Science and product vision for terrestrial global change research. *Remote Sensing of Environment* **2014**, *145*, 154-172.
34. Wulder, M.A.; White, J.C.; Goward, S.N.; Masek, J.G.; Irons, J.R.; Herold, M.; Cohen, W.B.; Loveland, T.R.; Woodcock, C.E. Landsat continuity: Issues and opportunities for land cover monitoring. *Remote Sensing of Environment* **2008**, *112*, 955-969.
35. Masek, J.G.; Vermote, E.F.; Saleous, N.E.; Wolfe, R.; Hall, F.G.; Huemmrich, K.F.; Gao, F.; Kutler, J.; Lim, T.K. A landsat surface reflectance dataset for north america, 1990-2000. *Ieee Geoscience and Remote Sensing Letters* **2006**, *3*, 68-72.
36. Vermote, E.F.; El Saleous, N.; Justice, C.O.; Kaufman, Y.J.; Privette, J.L.; Remer, L.; Roger, J.C.; Tanré, D. Atmospheric correction of visible to middle-infrared eos-modis data over land surfaces: Background, operational algorithm and validation. *Journal of Geophysical Research D: Atmospheres* **1997**, *102*, 17131-17141.
37. Xiao, X.; Biradar, C.M.; Czarnecki, C.; Alabi, T.; Keller, M. A simple algorithm for large-scale mapping of evergreen forests in tropical america, africa and asia. *Remote Sensing* **2009**, *1*, 355-374.
38. Tucker, C.J. Red and photographic infrared linear combinations for monitoring vegetation. *Remote Sensing of Environment* **1979**, *8*, 127-150.
39. Huete, A.; Didan, K.; Miura, T.; Rodriguez, E.P.; Gao, X.; Ferreira, L.G. Overview of the radiometric and biophysical performance of the modis vegetation indices. *Remote Sensing of Environment* **2002**, *83*, 195-213.
40. Xiao, X.; Hollinger, D.; Aber, J.; Goltz, M.; Davidson, E.A.; Zhang, Q.; Moore Iii, B. Satellite-based modeling of gross primary production in an evergreen needleleaf forest. *Remote Sensing of Environment* **2004**, *89*, 519-534.
41. Potere, D.; Feierabend, N.; Strahler, A.H.; Bright, E.A. Wal-mart from space: A new source for land cover change validation. *Photogrammetric Engineering and Remote Sensing* **2008**, *74*, 913-919.
42. Kou, W.; Xiao, X.; Dong, J.; Gan, S.; Zhai, D.; Zhang, G.; Qin, Y.; Li, L. Mapping deciduous rubber plantation areas and stand ages with palsar and landsat images. *Remote Sensing* **2015**, *7*, 1048-1073.
43. Benz, U.C.; Hofmann, P.; Willhauck, G.; Lingenfelder, I.; Heynen, M. Multi-resolution, object-oriented fuzzy analysis of remote sensing data for gis-ready information. *Isprs Journal of Photogrammetry and Remote Sensing* **2004**, *58*, 239-258.
44. Bajocco, S.; Dragoz, E.; Gitas, I.; Smiraglia, D.; Salvati, L.; Ricotta, C. Mapping forest fuels through vegetation phenology: The role of coarse-resolution satellite time-series. *PLoS ONE* **2015**, *10*, e0119811.

45. Kavzoglu, T.; Yildiz, M. Parameter-based performance analysis of object-based image analysis using aerial and quikbird-2 images. *ISPRS Ann. Photogramm. Remote Sens. Spatial Inf. Sci.* **2014**, *II-7*, 31-37.
46. Mallinis, G.; Koutsias, N.; Tsakiri-Strati, M.; Karteris, M. Object-based classification using quickbird imagery for delineating forest vegetation polygons in a mediterranean test site. *ISPRS Journal of Photogrammetry and Remote Sensing* **2008**, *63*, 237-250.
47. Liu, D.; Xia, F. Assessing object-based classification: Advantages and limitations. *Remote Sensing Letters* **2010**, *1*, 187-194.
48. Li, P.; Zhang, J.; Feng, Z. Mapping rubber tree plantations using a landsat-based phenological algorithm in xishuangbanna, southwest china. *Remote Sensing Letters* **2015**, *6*, 49-58.
49. Fan, H.; Fu, X.H.; Zhang, Z.; Wu, Q. Phenology-based vegetation index differencing for mapping of rubber plantations using landsat oli data. *Remote Sensing* **2015**, *7*, 6041-6058.
50. Tan, Z.; Zhang, Y.; Song, Q.; Yu, G.; Liang, N. Leaf shedding as an adaptive strategy for water deficit: A case study in xishuangbannas rainforest. *Journal of Yunnan University. Natural Science* **2014**, *36*, 273-280.
51. Zhou, W.; Sha, L.; Shen, S.; Zheng, Z. Seasonal change of soil respiration and its influence factors in rubber (*hevea brasiliensis*) plantation in xishuangbanna, sw china. *Journal of Mountain Science* **2008**, 317-325.
52. Dong, J.; Xiao, X.; Kou, W.; Qin, Y.; Zhang, G.; Li, L.; Jin, C.; Zhou, Y.; Wang, J.; Biradar, C.; Liu, J.; Moore Iii, B. Tracking the dynamics of paddy rice planting area in 1986–2010 through time series landsat images and phenology-based algorithms. *Remote Sensing of Environment* **2015**, *160*, 99-113.
53. Liu, J.-J.; Slik, J.W.F. Forest fragment spatial distribution matters for tropical tree conservation. *Biol. Conserv.* **2014**, *171*, 99-106.
54. Priyadarshan, P. *Biology of hevea rubber*. CABI: 2011.
55. Ming, D.; Li, J.; Wang, J.; Zhang, M. Scale parameter selection by spatial statistics for geobia: Using mean-shift based multi-scale segmentation as an example. *Isprs Journal of Photogrammetry and Remote Sensing* **2015**, *106*, 28-41.
56. Drăguţ, L.; Schauppenlehner, T.; Muhar, A.; Strobl, J.; Blaschke, T. Optimization of scale and parametrization for terrain segmentation: An application to soil-landscape modeling. *Computers & Geosciences* **2009**, *35*, 1875-1883.
57. Dragut, L.; Tiede, D.; Levick, S.R. Esp: A tool to estimate scale parameter for multiresolution image segmentation of remotely sensed data. *International Journal of Geographical Information Science* **2010**, *24*, 859-871.
58. Emary, E.; Mostafa, K.; Onsi, H.; Ieee. *A proposed multi-scale approach with automatic scale selection for image change detection*. 2009; p 3185-3188.
59. Karl, J.W.; Maurer, B.A. Spatial dependence of predictions from image segmentation: A variogram-based method to determine appropriate scales for producing land-management information. *Ecological Informatics* **2010**, *5*, 194-202.